NMR Structure and Dynamics of the C-Terminal Domain from Human Rev1 and Its Complex with Rev1 Interacting Region of DNA Polymerase #

Published in final edited form as:
Biochemistry. 2012 July 10; 51(27): 5506–5520. doi:10.1021/bi300566z.

NMR Structure and Dynamics of the C-terminal Domain from Human Rev1 and its Complex with Rev1 Interacting Region of DNA Polymerase η

Alexandra Pozhidaeva[a,†], **Yulia Pustovalova**[a,†], **Sanjay D'Souza**[b], **Irina Bezsonova**[a], **Graham C. Walker**[b], and **Dmitry M. Korzhnev**[a,*]

[a]Department of Molecular, Microbial and Structural Biology, University of Connecticut HealthCenter, Farmington, CT 06030, USA

[b]Department of Biology, Massachusetts Institute of Technology, Cambridge, MA 02139, USA

Abstract

Rev1 is a translesion synthesis (TLS) DNA polymerase essential for DNA damage tolerance in eukaryotes. In the process of TLS stalled high-fidelity replicative DNA polymerases are temporarily replaced by specialized TLS enzymes that can bypass sites of DNA damage (lesions), thus allowing replication to continue or postreplicational gaps to be filled. Despite its limited catalytic activity, human Rev1 plays a key role in TLS by serving as a scaffold that provides an access of Y-family TLS polymerases polη, ι, and κ to their cognate DNA lesions and facilitates their subsequent exchange to polζ that extends the distorted DNA primer-template. Rev1 interaction with the other major human TLS polymerases, polη, ι, κ and the regulatory subunit Rev7 of polζ, is mediated by Rev1 C-terminal domain (Rev1-CT). We used NMR spectroscopy to determine the spatial structure of the Rev1-CT domain (residues 1157-1251) and its complex with Rev1 interacting region (RIR) from polη (residues 524-539). The domain forms a four-helix bundle with a well-structured N-terminal β-hairpin docking against helices 1 and 2, creating a binding pocket for the two conserved Phe residues of the RIR motif that upon binding folds into an α-helix. NMR spin-relaxation and NMR relaxation dispersion measurements suggest that free Rev1-CT and Rev1-CT/polη-RIR complex exhibit μs-ms conformational dynamics encompassing the RIR binding site, which might facilitate selection of the molecular configuration optimal for binding. These results offer new insights into the control of TLS in human cells by providing a structural basis for understanding the recognition of the Rev1-CT by Y-family DNA polymerases.

Introduction

Reactive products of cellular metabolism and external genotoxic agents such as ultraviolet (UV) irradiation cause persistent damage to the genomic DNA, which is constantly removed

*Corresponding author: Dmitry M. Korzhnev, Phone: (860) 679 2849, Fax: (860) 679 3408, korzhniev@uchc.edu.
†Shared first authorship

Data Deposition: Atomic coordinates of the Rev1-CT domain and the Rev1-CT/polh-RIR complex were deposited to Protein Data Bank (PDB entries 2LSY, 2LSK). The backbone and side chain NMR resonance assignments were deposited to BioMagResBank (BMRB entries 18455, 18434).

Supporting Information: Supplementary Figure 1S with ^{1}H-^{1}H cross-sections from a ^{13}C-edited ^{15}N,^{13}C-filtered NOESY-HSQC spectrum of Rev1-CT/polη-RIR complex, displaying intermolecular protein-peptide NOE cross-peaks between selected groups of $^{13}C/^{15}N$ labeled Rev1-CT domain and ^{1}H nuclei of the unlabeled polη-RIR peptide. Supplementary Figure 2S with examples of ^{15}N CPMG relaxation dispersion data fits for selected residues of Rev1-CT/polη-RIR complex, and a plot illustrating ^{15}N chemical shift differences obtained from ^{15}N CPMG relaxation dispersion data for Rev1-CT/polη -RIR complex, $\Delta\omega_{disp}$, and ^{15}N chemical shift differences between free and polη-RIR bound forms of Rev1-CT domain, $\Delta\omega_{spec}$. This material is available free of charge via the Internet at http://pubs.acs.org.

through various DNA repair mechanisms[1]. Unavoidably, however, some DNA modifications (lesions) are present during S-phase, creating blocks for progression of the DNA replication machinery since spatially constrained active sites of high-fidelity replicative DNA polymerases cannot accommodate most types of DNA damage. To circumvent this problem, organisms in all kingdoms of life have evolved DNA damage tolerance pathways employing specialized translesion synthesis (TLS) DNA polymerases that can insert nucleotides across DNA lesions, thereby allowing replication to proceed while temporarily leaving DNA damage unrepaired[2-7]. Growing evidence suggests that an additional important component of TLS DNA polymerase action is to fill postreplicational gaps opposite lesions at the end of the cell cycle so that double strand breaks are not generated during the next round of DNA replication [8-12].

The most intensively studied TLS polymerases are the Y-family enzymes Rev1, polη, polι polκ and the B-family polymerase polζ (a complex of the catalytic Rev3 subunit with Rev7)[2-7]. TLS polymerases lack 3′→5′ proofreading exonuclease activity, possess more accommodating active sites than replicative DNA polymerases, and make a relatively limited number of contacts with the template base and incoming nucleotide[13]. These features allow them to insert nucleotides across from a wide variety of DNA lesions that would stall a replicative DNA polymerase. However, the ability to replicate through altered bases comes at an expense of fidelity. The nucleotide misincorporation rates of TLS polymerases copying undamaged DNA are *ca.* 10^{-1}-10^{-4}, much higher than the misincorporation rates of 10^{-6} -10^{-8} observed for polδ and polε, the main replicative DNA polymerases[2,3,14]. Consequently, the access of these error-prone TLS enzymes to primer termini is carefully regulated.

Certain TLS polymerases are specialized for the efficient and relatively accurate insertion of nucleotides opposite particular lesions [5-7], termed cognate lesions. Examples of cognate lesions include thymine-thymine cyclobutane pyrimidine dimers (T-T CPDs) for polη[15,16] and N^2-dG adducts, such as N^2-benzo[a]pyrene-dG (BaP-dG) adducts, for polκ[17,18]. Although these TLS polymerases can also replicate over certain non cognate lesions as well, they do so in a more error-prone manner. Furthermore, the bypass of many DNA lesions, including bulky BaP-dG adducts, cisplatin (cisPt) adducts, and [6-4] photoproducts ([6-4]PP), is accomplished *via* the coordinated consecutive action of two different TLS DNA polymerases[19-21]. An inserter TLS polymerase (e.g. polη, ι or κ) incorporates a nucleotide across the site of DNA damage. This inserter polymerase is then replaced by another TLS enzyme that extends from the distorted primer terminus positioned across from the lesion. This extender role is frequently carried out by polζ, which is recruited to the primer terminus in a process mediated by Rev1[3,22,23]. Rev1/polζ-dependent TLS is responsible for most of the DNA damage-induced mutagenesis in eukaryotic cells and contributes to spontaneous mutagenesis as well[22,23]. On the other hand, certain DNA lesions such as cyclobutane pyrimidine dimers (CPDs) or abasic sites can be effectively bypassed by a single TLS enzyme. For example, polη alone can efficiently replicate through T-T CPD, one of the common types of UV induced lesions, in an essentially error-free manner[15,16]. Xeroderma pigmentosum variant (XPV) individuals, who lack polη function are highly UV-sensitive and cancer-prone[16]. They exhibit increased UV-induced mutagenesis due to more error-prone polymerases carrying out TLS in the absence of the more accurate polη[24].

Protein-protein interactions play critical roles in controlling the access of TLS polymerases to their cognate DNA lesions and facilitating polymerase switching during bypass replication[4-7]. Beyond their catalytic cores, Y-family TLS enzymes possess auxiliary domains and motifs that are important for their efficient interactions with one another and with the DNA[5-7]. TLS polymerases possess ubiquitin-binding motif (UBM) or ubiquitin-

binding zinc finger (UBZ) domains in addition to the proliferating cell nuclear antigen (PCNA) interacting motifs[25]. These ubiquitin-binding domains play a role in the recruitment of TLS DNA polymerases to PCNA processivity clamps that have been mono-ubiquitinated at Lys164 in a Rad6/Rad18-dependent fashion in response to DNA damage[26]. The PCNA-interacting protein (PIP) box motifs of polη, ι, and κ additionally contribute to the interaction with mono-ubiquitinated PCNA, while Rev1, which lacks a consensus PIP-box motif, instead utilizes its N-terminal BRCT (BRCA1 C-terminus), its polymerase associated (PAD) or UBM domains for PCNA binding[27-29]. In addition, as discussed in the detail in this paper, the C-terminal parts of vertebrate polη, ι, κ contain Rev1-interacting regions (RIRs), consisting of short peptide motifs containing two consecutive phenylalanines that bind to the Rev1 C-terminal domain (Rev1-CT)[30].

The human Y-family Rev1 polymerase is a 1251 amino acid (aa) protein that is notable for its role, along with polζ, in most DNA damage induced mutagenesis[31-33]. The Rev1 catalytic activity, however, is limited to inserting dCMP opposite a G template or certain types of DNA lesions, and thus is insufficient to explain its role in introducing mutations[33-35]. Subsequent studies revealed that Rev1 possesses a “second function” besides its catalytic ability that is important for TLS and mutagenesis[36]. This second, and more important, function of Rev1 proved to be the recruitment and coordination of other DNA polymerases during the process of TLS *via* specific protein-protein interactions[5-7]. Thus, Rev1 serves as a scaffold that provides access for the Y-family polymerases η,ι, and κ to their cognate DNA lesions, and can also facilitate the subsequent exchange to polζ, which then extends the distorted DNA primer terminus opposite the lesion. Remarkably, previous studies of intermolecular interactions of Rev1 fragments using yeast two-hybrid assays, co-immuno precipitation and cellular co-localization revealed that Rev1's interaction with the other three Y-family TLS polymerases, polη, ι, and κ, and with polζ as well is mediated by a relatively small 100 aa Rev1-CT domain[30,37,39]. The human Y-family polymerases η, ι and κ bind the Rev1-CT with RIR peptide motifs that contain two consecutive Phe residues[30]. Such motifs are absent in the Rev3 and Rev7 subunits of polζ also known to interact with the Rev1-CT in vertebrates[37-40], suggesting that their mode of Rev1-CT binding is different from that of polymerases η, ι and κ. Previous reports suggest that the loss of *S. cerevisiae* Rev1-CT has a detrimental effect on cell survival and results in a decrease of mutagenesis after DNA damage[41]. Although the crystal structure of the central polymerase domain of both human and yeast Rev1 have been solved, the critically important protein-protein interaction Rev1-CT domain was removed to facilitate crystallization[42,43].

The versatility of Rev1-CT interactions renders characterization of this module critical for understanding the underlying mechanisms of TLS. Here we report high-resolution spatial structures of human Rev1-CT domain (residues 1157-1251) and its complex with Rev1 interacting region (RIR) from polη (residues 524-539) determined by solution NMR spectroscopy, as well as a detailed characterization of conformational flexibility of the free Rev1-CT domain and the complex on various time-scales using ^{15}N NMR spin-relaxation[44] and ^{15}N NMR relaxation dispersion measurements[45]. The functional importance of particular amino acids to this interaction is demonstrated through the use of yeast two-hybrid analysis. Taken together, these data provide a rigorous structural basis for understanding Rev1 interactions with human Y-family TLS polymerases.

Experimental Procedures

Protein sample preparation for NMR spectroscopy

The gene encoding human Rev1-CT domain (residues 1158-1251 of Rev1 inserted after the cleavage site for TEV protease - ENLYFQG), codon optimized for expression in *E. coli,*

was custom synthesized (GenScript) and sub-cloned into pET-28b(+) vector (Novagen) using NdeI -BamHI restriction sites.

The recombinant human Rev1-CT was over-expressed in *E. coli* BL21 (DE3) cells. $^{15}N/^{13}C$ labeled protein for NMR spectroscopy was produced by growing cells transformed with Rev1-CT plasmid in minimal M9 medium using $^{15}NH_4Cl$ and ^{13}C-glucose as sole nitrogen and carbon sources, respectively. Cells were grown at 37 °C to OD_{600} of 0.6-0.8 followed by induction of protein expression by 1 mM IPTG overnight at 20 °C. After harvesting, the bacterial pellets were re-suspended in loading buffer containing 50 mM NaH_2PO_4, 250 mM NaCl, 10 mM imidazole, 1 mM PMSF, pH 7.4. After the cells were lysed by sonication, the soluble fraction was loaded onto a Ni^{2+} affinity column and incubated for 1 h at 4°C. After an extensive wash with the loading buffer, the protein was eluted with the buffer of the same composition, but containing 250 mM imidazole. The His-tag was removed by TEV cleavage for 4 h at 20°C or overnight at 4°C in the presence of 2 mM DTT and 0.5 mM EDTA, followed by protein purification on a HiLoad Superdex 75 column (GE Healthcare). After concentration, the final sample of free Rev1-CT domain contained 0.9 mM $^{15}N/^{13}C$ labeled protein, 50 mM NaH_2PO_4, 100 mM NaCl, 0.25 mM EDTA, 5 mM DTT, 0.05% NaN_3, 10% D_2O, pH 7.0. Protein cleavage with TEV protease leaves an N-terminal Gly residue, so that the resulting Rev1-CT domain included residues 1157-1251 of human Rev1 with Pro1157 mutated to Gly. The consistency of the protein sample was confirmed by MALDI-TOF mass spectroscopy.

The complex of $^{15}N/^{13}C$ labeled Rev1-CT domain with custom synthesized (GenScript) 16 aa unlabeled peptide that encompasses one of the two RIR regions of polη (residues 524-539; QSTGTEP**FF**KQKSLLL)[30] was prepared by gradually titrating 25 mM peptide solution into 0.9 mM protein sample. The binding was monitored by recording ^{1}H-^{15}N HSQC spectra at each step of the titration. The final sample of the complex contained 0.9 mM $^{15}N/^{13}C$ Rev1-CT - unlabeled polη-RIR mixed in 1:1 molar ratio, 50 mM NaH_2PO_4, 100 mM NaCl, 0.25 mM EDTA, 5 mM DTT, 0.05% NaN_3, 10% D_2O, pH 7.0. At this protein concentration, about 89% of the protein and the peptide are in the bound state, estimated assuming dissociation constant K_D = 13 μM for the complex reported in previous studies[30].

NMR resonance assignment and protein structure calculation

NMR spectra for the free $^{15}N/^{13}C$ Rev1-CT domain and its complex with the unlabeled polη-RIR peptide were collected at 15 °C on Agilent VNMRS spectrometers equipped with cold probes operating at 11.7 and 18.8 T magnetic fields (500 and 800 MHz ^{1}H frequencies). The backbone and side-chain ^{15}N, ^{13}C and ^{1}H resonances of Rev1-CT domain were assigned from 2D ^{1}H-^{15}N HSQC, ^{1}H-^{13}C HSQC and 3D HNCA, HNCACB, HNCO, HBHA(CO)NH, HC(C)H-TOCSY, (H)CCH-TOCSY, ^{15}N-edited NOESY-HSQC and ^{13}C-edited NOESY-HSQC (150 ms mixing time) spectra[46]. Two sets of experiments were performed (i) for the free $^{15}N/^{13}C$ Rev1-CT domain and (ii) for $^{15}N/^{13}C$ Rev1-CT - unlabeled polη-RIR complex. The assignments of ^{1}H NMR resonances for polη-RIR peptide in complex with $^{15}N/^{13}C$ Rev1-CT domain were obtained from 2D ^{15}N,^{13}C-filtered TOCSY, COSY and NOESY (250 ms mixing time) spectra[47], containing intra-molecular ^{1}H-^{1}H correlations from the unlabeled peptide, collected in both 90% H_2O/10% D_2O and in 100% D_2O buffers (COSY spectrum was recorded in D_2O buffer only). In addition, we have recorded 3D ^{13}C-edited ^{15}N, ^{13}C-filtered NOESY-HSQC spectrum, containing inter-molecular NOE correlations between $^{15}N/^{13}C$ Rev1-CT domain and the unlabeled polη-RIR peptide used for structure determination of the complex[47]. NMR spectra were processed with NMRPipe[48] and analyzed with CARA software[49]. Nearly complete

backbone 95%(94%) and side-chain 90%(90%) resonance assignments were obtained for the free Rev1-CT domain (the complex).

Structure calculations for the Rev1-CT domain and Rev1-CT/polη-RIR complex were performed in CYANA software[50]. The restraints for the backbone dihedral φ and ψ angles were derived from the backbone ^{1}H,^{15}N and ^{13}C chemical shifts using TALOS+ program[51]. Intra-molecular ^{1}H-^{1}H distance restraints for the free and bound forms of Rev1-CT were obtained from 3D ^{15}N- and ^{13}C-edited NOESY-HSQC spectra, while inter-molecular distance restraints and restraints within the polη-RIR peptide were derived from 3D ^{13}C-edited ^{15}N, ^{13}C-filtered NOESY-HSQC and 2D ^{15}N, ^{13}C-filtered NOESY experiments, respectively. Intra-molecular NOE correlations for Rev1-CT domain in free and bound states were assigned automatically in CYANA, while protein-peptide and inter-peptide NOEs were assigned manually. Hydrogen bond restraints were added on the basis of NOE analysis. A total of 200 structures of the free Rev1-CT domain and the complex were generated, followed by refinement of 20 final lowest-energy structures by short constrained molecular dynamic simulations in explicit solvent using CNS software[52]. Table 1 summarizes NMR based restraints used for structure calculation of Rev1-CT domain and the complex along with structure refinement statistics.

NMR characterization of protein dynamics

The backbone ^{15}N R_1, R_2 (CPMG) and $^{15}N\{^{1}H\}$ NOE NMR relaxation measurements for the Rev1-CT domain and its complex with polη -RIR peptide were performed at 11.7 T Agilent VNMRS spectrometer at 15 °C using the pulse-sequences of Farrow et al.[53]. The delay between 180° refocusing pulses of CPMG sequence in ^{15}N R_2 experiment was set to δ = 1 ms, corresponding to CPMG frequency $\nu_{CPMG} = 1/(2\delta)$ of 500 Hz. ^{15}N R_1 and R_2 rates and their uncertainties were obtained from exponential fits of peak intensities in a series of 8 2D ^{1}H-^{15}N correlation spectra recorded at different relaxation delays. ^{15}N R_2 rates were numerically corrected to take into account small systematic contributions due to off-resonance effects of CPMG refocusing pulses[54]. $^{15}N\{^{1}H\}$ NOE values were calculated as ratios of peak intensities in corresponding 2D ^{1}H-^{15}N correlation spectra recorded with and without ^{1}H saturation using 8 s delay between scans to ensure full recovery of ^{15}N longitudinal magnetization. To account for possible systematic uncertainties in measured NMR relaxation data the minimal errors of 2% for ^{15}N R_1, R_2 rates and 0.05 for $^{15}N\{^{1}H\}$ NOE values were assumed.

Overall rotation diffusion tensors for the free Rev1-CT domain and Rev1-CT/polη-RIR complex and overall rotation correlation time $\tau_R = 1/(2(D_x+D_y+D_z))$ (D_i, i = x,y,z are eigenvalues of rotation diffusion tensor) were calculated from ^{15}N R_1 and R_2 data using the program DASHA[55]. Specifically, ^{15}N R_1 and R_2 rates were globally fit to the models assuming isotropic, axially symmetric and fully anisotropic rotational diffusion tensor[44]. Included in these calculations were the residues with (i) non-overlapped cross-peaks in ^{1}H-^{15}N correlation spectra, (ii) $^{15}N\{^{1}H\}$ NOE > 0.6 and (iii) ^{15}N R_2/R_1 ratios within mean ± 2 standard deviations. In both cases the model of axially symmetric anisotropic rotation diffusion was selected according to F- test at 10% significance level, resulting in τ_R = 8.96±0.07 ns (10.45±0.06 ns) and $D_x/D_z = D_y/D_z$ = 0.91±0.02 (0.84±0.01) for the free Rev1-CT domain (Rev1-CT/polη-RIR complex).

Pico- to nanosecond conformational dynamics of Rev1-CT domain in free and bound forms were assessed from the analysis of ^{15}N relaxation data using Lipari-Szabo model-free approach[44,56], performed in DASHA software[55]. At this stage of the data analysis the parameters of molecular overall rotation were fixed to previously determined values, and ^{15}N R_1, R_2 and $^{15}N\{^{1}H\}$ NOE data were fit on a per-residue basis using the models of spectral density function including the following adjustable parameters: (i) $\{S^2\}$, (ii) $\{S^2$,

τ_e}, (iii) {S^2, R_{ex}}, (iv) {S_f^2, S_s^2, τ_s} and (v) {S^2, τ_e, R_{ex}}, where S^2, S_f^2 and S_s^2 ($S_2=S_f^2S_s^2$) are generalized order parameters describing angular amplitudes of internal motions of N-H vectors, τ_e, τ_s are correlation times for fast ps and slower ns time-scale internal motions, R_{ex} (below referred to as $R_{ex,mf}$) is contribution to transverse relaxation rate R_2 due to μs-ms conformational exchange. Model selection was performed based on the values of χ^2 penalty function, describing goodness of relaxation data fit, according to the protocol of Mandel et al.[57] (significance levels of 5% and 20%, respectively, were assumed for χ^2 and F-test).

The residues in free Rev1-CT domain and its complex with polη-RIR peptide exhibiting *micro- to millisecond conformational exchange* were identified based on $R_{ex,mf}$ values obtained in model-free analysis of ^{15}N relaxation data[44,56]. CPMG sequence used in ^{15}N R_2 experiment suppresses exchange contribution to R_2 provided that $2\pi\nu_{CPMG} \gg k_{ex}$ and $2\pi\nu_{CPMG} \gg \Delta\omega$, where k_{ex} and $\Delta\omega$ are exchange rate constant and frequency difference between the exchanging states[58]. Therefore, $R_{ex,mf}$ primarily reflect contributions to R_2 due to *fast μs-ms conformational exchange* with $k_{ex} \geq 2\pi\nu_{CPMG}$ accompanied by changes in NMR chemical shifts. To quantify R_{ex} contributions to ^{15}N R_2 due to *slower ms time-scale exchange* we have performed ^{15}N CPMG relaxation dispersion measurements[45,59], where the effective transverse relaxation rates $R_{2,eff}$ were obtained as a function of ν_{CPMG}. ^{15}N relaxation dispersion profiles for the free Rev1-CT and Rev1-CT/polη-RIR complex were recorded at 11.7 T (the free domain and the complex) and 18.8 T (the complex only) magnetic fields with the pulse-sequence of Hansen et al.[60], using a constant relaxation period T = 30 ms and ν_{CPMG} ranging from 33 to 1000 Hz. Relaxation dispersion data measured at 11.7 T were least-square fit to a model of two-state conformational exchange as described elsewhere[61]. The best-fit dependencies $R_{2,eff}^{clc}(\nu_{CPMG})$ were used to estimate exchange contributions $R_{ex,rd} = R_{2,eff}^{clc}(33Hz)-R_{2,eff}^{clc}(533Hz)$ to ^{15}N R_2 that complement model-free derived $R_{ex,mf}$ measured at ν_{CPMG} of 500 Hz.

Yeast two-hybrid analysis

Studies of protein-protein interactions in the yeast two-hybrid system were performed in the PJ69-4A strain of yeast[62]. DNA fragments encoding the C-terminal fragment of human Rev1 (amino acids from 1131-1249) and full-length human polη (amino acids from 1-713), were subcloned into the pGAD-C1 (*GAL4* AD) and the pGBD-C1 (*GAL4* BD) plasmids marked with leucine and tryptophan respectively. The assay was performed by growing strains harboring the two plasmids in 3 ml of media lacking leucine and tryptophan for 2 days at 30°C and spotting 5μL of cells on selective media plates lacking leucine and tryptophan (-LW) and on medium also lacking adenine and histidine (-AHLW) to score positive interactions. Interactions were scored after 3 days of growth at 30 °C.

Site-directed mutations for yeast two-hybrid analysis were generated according to the protocol of the Quikchange Mutagenesis kit (Stratagene), except that we used an annealing temperature of 50 °C and an extension time of 2min/kb. Mutations were verified by sequencing.

Results and Discussion

The Rev1 C-terminus is a structured domain that binds human Y-family DNA polymerases

Previous studies established that the C-terminal ~100 aa region of DNA polymerase Rev1 (Rev1-CT) is critical for DNA damage tolerance in eukariotes[37-39]. However, removal of a fragment of Rev1 containing this region does not alter the dCMP transferase activity of yeast Rev1 *in vitro*[63], supporting the notion that Rev1 plays a non-catalytic, structural role in translesion synthesis (TLS) by coordinating the action of other TLS polymerases through protein-protein interactions[4-7,64]. The binding of human and mouse Rev1-CT domain with

each of the other vertebrate Y-family polymerases, polη, ι κ, and with Rev7, the regulatory subunit of polζ has been demonstrated by multiple experimental techniques, including yeast two-hybrid assays, co-immuno precipitation, and cellular co-localization[30,37-39]. Although the Rev1-CT domain is highly conserved in eukaryotes, its ability to bind other Y-family DNA polymerases has only evolved in higher organisms[65], in contrast to the Rev1-CT/Rev7 interaction, which has been reported in eukaryotes from yeast to humans[5]. Secondary structure prediction and sequence alignment of Rev1-CT from different species suggested that the domain likely consists of four amphipathic helices, which would have the potential for forming a four-helix bundle, and identified several conserved motifs that seemed likely to be involved in the hydrophobic core of the domain and whose mutation impairs the function of yeast *REV1* gene *in vivo*[41].

Despite the wealth of biochemical and mutational data, the detailed atomic-level picture of Rev1-CT interactions with other TLS polymerases has remained obscure due to the lack of a high-resolution spatial structure of the domain. In order to determine the solution NMR structure of the human Rev1-CT domain (residues 1157-1251) we have expressed and purified $^{15}N/^{13}C$ labeled protein and performed its backbone and side-chain resonance assignment using a standard set of triple-resonance NMR experiments[46]. Figure 1A shows ^{1}H-^{15}N HSQC spectrum of the free Rev1-CT domain (red) recorded at 11.7 T field at 15 °C, revealing a single set of well dispersed NMR resonances indicative of a structured protein domain. NMR chemical shifts obtained at this stage of the data analysis provide a plentiful source of information on local protein structure and conformational dynamics. Thus, secondary structure prediction based on the backbone ^{1}H,^{15}N and ^{13}C chemical shifts using TALOS+ program[51] (Figure 1B, red) confirmed that the domain consists of four a-helices, referred to below as H1 to H4. Order parameters S^2 for the backbone amide groups of the free Rev1-CT (Figure 1C, red) that describe the main chain conformational flexibility (S^2=1 for fully restricted, 0 for unconstrained motions) were empirically predicted from the backbone chemical shifts using Random Coil Index (RCI) approach[66,67]. High S^2 observed throughout the protein sequence suggest rather limited mobility of the domain on ps-ns to μs time-scale[67]. In contrast, the free Rev1-CT domain seems to be dynamic on a time-scale from μs to ms. At temperatures above 20-25 °C the quality of Rev1-CT spectra deteriorate significantly due to extensive line-broadening indicative of μs-ms conformational exchange. Decreasing the temperature to 15 °C improves spectra quality, although the resonances from loops between helices H1-H2 and H3-H4 still remain broadened, some beyond the level of detection.

The Rev1-CT domain has been previously shown to form medium to weak affinity complexes with short peptide motifs (Rev1 interacting regions, RIRs) from human Y-family DNA polymerases η, ι and κ containing two consecutive Phe residues (Figure 1D) with dissociation constants (K_D) ranging from 8 to 69 μM[30]. One RIR motif was identified in each of human polι and polκ, while two motifs were found in human polη (Figure 1D). In order to elucidate the structural basis for Rev1-CT interactions with human Y-family DNA polymerases, we have performed NMR studies of the Rev1-CT complex with a 16 amino acid peptide containing one of the two RIR motifs of human polη (residues 524-539, line 1 in Figure 1D). Figure 1A shows ^{1}H-^{15}N HSQC spectrum of the Rev1-CT/polη-RIR complex (blue) superimposed on the spectrum of the free domain (red). The backbone and side-chain NMR resonance assignments for $^{15}N/^{13}C$ labeled Rev1-CT in complex with the unlabeled polη peptide were obtained as described above for the free domain, while ^{1}H resonances of the peptide were assigned from a set of filtered 2D ^{1}H-^{1}H experiments. The analysis of the backbone ^{1}H,^{15}N and ^{13}C chemical shifts of Rev1-CT domain bound to polη-RIR peptide suggests that neither secondary structure (Figure 1B, blue) nor backbone amide order parameters S^2 that report on main chain dynamics (Figure 1C, blue) change significantly upon the complex formation. On the other hand, NMR resonances from H1-H2

and H3-H4 loops exhibit somewhat less broadening due to μs-ms conformational exchange. Chemical shift changes upon the complex formation are observed in the region of the Rev1-CT domain comprising helices H1 and H2, as well as in the N-terminal part preceding helix H1, suggesting that this part of the domain is involved in Y-family polymerase binding.

Titrations of Rev1-CT domain with increasing amounts of polη -RIR peptide monitored by ^{1}H- ^{15}N HSQC spectra suggest that the binding process is slow on the NMR time-scale. Namely, peaks corresponding to free Rev1-CT decrease in intensity and ultimately disappear, while peaks of the bound form show up in new places in spectra and increase in intensity with increasing the peptide concentration (as illustrated in the inset to Figure 1A for Leu 1171). In the case of two-state chemical exchange between equally populated states, two peaks are observed in the NMR spectrum of a nucleus if the forward and reverse rates *k* for the process are slower than $\Delta\omega/2^{3/2}$ (coalescence point), where δω is frequency difference between the exchanging states[68]. Separate peaks as close as 0.03 ppm (^{1}H) corresponding to free and bound Rev1-CT are observed in 11.7 T ^{1}H-^{15}N HSQC spectra recorded at about 1:0.5 protein/peptide ratio, suggesting that association $k_{on}[L]$ ([L] is concentration of free peptide) and dissociation k_{off} rates for Rev1-CT/polη-RIR interaction are slower than ~33 s^{-1}. Assuming the previously reported K_D = 13 μM[30] and total protein and peptide concentrations $[P_0]$ = 0.9 mM and $[L_0]$ = 0.45 mM, respectively, one can estimate the upper limit for k_{on} of Rev1-CT/polη-RIR association as $2.7 \cdot 10^6$ M^{-1} s^{-1}, which is of the same order of ~10^6 M^{-1} s^{-1} expected for diffusion controlled protein association[69]. This observation suggests that the Rev1-CT/polη-RIR association is likely somewhat slower than diffusion controlled, potentially pointing to a barrier crossing event due to rearrangements of interaction partners.

Structure of the free Rev1-CT domain

Figure 2 shows the spatial structure of the human Rev1-CT domain (residues 1157-1251) as determined by solution NMR spectroscopy. The ensemble of 20 least-energy structures of the domain (Figure 2A) is in excellent agreement with the input experimental data, displaying mean pairwise RMSD for the backbone atoms of regular secondary structure elements of 0.53 Å, and exhibiting minimal violations of distance/torsion angle restraints and deviations from idealized molecular geometry (Table 1). As expected, the domain adopts a four-helix bundle fold with helices H1, H2, H3 and H4 spanning the residues 1165-1178, 1184-1199, 1203-1219 and 1224-1243, respectively (Figure 2B). The N-terminal 8 residues (1157-1164) of the domain preceding α-helix H1 form a rigid type I′ β-hairpin stabilized by two hydrogen bonds between Leu 1159 and Ala 1162 (NH_{1159}-CO_{1162}, CO_{1159}-NH_{1162}). The β-hairpin tightly packs against helices H1 and H2, resulting in multiple long-range NOE contacts between Leu 1159 - Val 1163 and Asn 1166, Asp 1167, Val 1168, Leu 1172 in α-helix H1, and between Leu 1159 and Gln 1189 in α- helix H2. Two hydrophobic residues in the β-turn, Ala 1160 and Gly 1161, together with hydrophobic side chains of Leu 1171, Trp 1175 from helix H1 and negatively charged Asp 1186 from helix H2 form a pocket on the surface of the domain (Figure 2C, left plot) capable of accommodating FF residues of RIR motifs of Y-type DNA polymerases (see below). It is notable that this region comprised of residues from the N-terminal β-hairpin and helices H1 and H2, exhibits the largest NMR chemical shift change upon polrη-RIR peptide binding. Figure 2C shows electrostatic charge distribution color mapped onto the surface of Rev1-CT domain. In addition to hydrophobic/negatively charged pocket described above located between helices H1 and H2 there is a large positively charged patch on the opposite side of the molecule formed by side-chains of Lys 1169 and Arg 1173 from helix H1 and Lys 1211, Lys 1214 and Arg 1215 from helix H3.

Side-chains of residues with solvent exposure less than 5% and an accessible surface area less than 10 $Å^2$ that form the core of the Rev1-CT domain are shown in Figure 2B and are

listed in the figure caption. Beyond side-chains buried in the hydrophobic core of the four-helix bundle, several residues form the interface between the N-terminal β-hairpin and α-helices H1 and H2. Recently, extensive sequence alignment of Rev1-CT domains from multiple eukaryotic species identified five conserved 5-6 residue regions within Rev1 C-terminus, referred to as *rev1-108* to *rev-112*[41]. Alanine-patch mutations of four of these regions (*rev1-108* - *rev1-111*) in yeast Rev1-CT completely abrogate the function of the *REV1* gene in cell survival after DNA damage induced by UV or methanesulfonate (MMS) exposure[41]. It is interesting to note that each of the *rev1-108, rev1-110* and *rev1-111* regions in the human Rev1-CT contain 2 to 4 residues from the core of the domain (see caption to Figure 2). Simultaneous mutations of multiple core residues, therefore may cause significant destabilization of the domain. Provided that the core of Rev1-CT is conserved among eukaryotic species, this observation explains why mutations of *rev1-108, rev1-110* and *rev1-111* in yeast are equivalent to loss of the whole domain, and, once again, underlines the importance of Rev1-CT domain for DNA damage tolerance in eukaryotes.

Structure of Rev1-CT/pol η-RIR complex

The finding that vertebrate Rev1-CT directly interacts with the three Y-family DNA polymerases, polη, ι and κ, sparked a search for Rev1 binding sequences (RIR motifs) in eukaryotic Y-family DNA polymerases[30, 37, 39]. This search proved non-trivial. As shown in Figure 1D, there is limited sequence homology among the four RIR regions found in human Y-family polymerases. Based on mutational analysis and truncations of RIR containing peptides Ohashi et al[30]. described the minimal RIR region as yyyFFxxxx (underlined in Figure 1D), where F is a phenylalanine residue, y is any amino-acid, and x is any amino acid but a proline. The two consecutive Phe residues are conserved among RIR regions, and substitution of any of them to Ala results in complete abrogation of RIR - Rev1-CT binding. In 3 of 4 RIRs found in human Y-family enzymes (Figure 1D) the FF sequence is preceded by Ser whose mutation in polκ decreases, but does not abolish Rev1-CT interaction[30]. Intriguingly, while there is no obvious sequence conservation in the region C-terminal to the FF motif, studies of the truncated RIR peptides suggest that at least four residues must follow the FF sequence in order to efficiently bind Rev1-CT. Mutation of any of the four residues to Ala has no effect on Rev1 interaction, yet substitution of any of them to Pro results in a complete loss of Rev1 interaction, suggesting that main chain conformation of RIR peptides is important for binding rather than specific side-chain contacts (beyond those formed by FF residues)[30].

To ascertain the mechanism of Rev1 recognition of Y-family DNA polymerases, we have determined the solution NMR structure of the Rev1-CT domain complex with an RIR containing peptide from human polη (residues 524-539) shown in Figure 3. The ensemble of 20 least-energy structures (Figure 3A) agrees well with the input experimental restraints (Table 1), exhibiting mean pairwise RMSD for the backbone atoms of regular secondary structure elements of 0.62 Å (Rev1-CT)/0.27 Å (polη peptide). Structure comparison of the free and bound forms of Rev1-CT domain (Figure 3B) reveal no noticeable structural changes in the domain upon polη-RIR binding. Interestingly, in the complex with Rev1-CT, the polη-RIR peptide forms an α-helix starting at Phe 531 and continuing all the way to the C-terminal Leu 539. The two phenylalanine residues, Phe 531 and Phe 532, are located in the first turn of the helix facing Rev1-CT domain surface. As anticipated from the mutational analysis of Rev1-CT/polκ-RIR interaction, the majority of contacts between Rev1-CT and polη -RIR peptide involve the two Phe residues, displaying extensive inter-molecular NOE connectivities in ^{13}C-edited ^{15}N,^{13}C-filtered NOESY-HSQC spectrum[47] (see supplementary Figure 1S). Both aromatic side-chains become buried upon Rev1-CT binding. The ring of Phe 532 deeply penetrates into the binding pocket on Rev1-CT surface formed by residues Ala 1160, Gly 1161 from the N-terminal β-turn, Leu 1171, Trp 1175

from helix H1, and Asp 1186, Gln 1189 from helix H2, while the ring of Phe 531 packs against Thr 1178 and Ile 1179 on the domain surface (Figure 3C,D). Notably, the pocket is already preformed in the free form of Rev1-CT domain (Figure 2C). As a result, Phe 531 and Phe 532 contribute 110 and 180 $Å^2$, respectively, to ~600 $Å^2$ interaction surface between Rev1-CT domain and polη-RIR peptide. The polη-RIR α-helix is tilted towards helices H1 and H2 of Rev1-CT (Figure 3A,B), with the backbone amides of Phe 531, Phe 532 and Lys 533 in the first turn of the α-helix facing the negatively charged surface of the Rev1-CT domain (Figure 2C). The key residue in Rev1-CT that interacts with the above amide groups of polη-RIR peptide is a highly conserved Asp 1186 from the helix H2, which is surface exposed in the free domain, but becomes completely buried upon the complex formation. Strikingly, as also discussed more fully below, mutation of the Asp 1186 to alanine completely eliminates the binding of the full-length polη to the Rev1-CT in the yeast two-hybrid system (Figure 4). The carboxyl of Asp 1186 side-chain participates in charge-dipole interactions with the backbone amides of Phe 531 (whose $^1H^N$ resonance is shifted to 11.1 ppm) and Phe 532 of polη-RIR peptide, and is also proximal to side-chain N^eH group of Trp 1175 and the backbone amide of Met 1183 from H1-H2 loop of Rev1-CT domain (Figure 3D). It is not an unusual feature for a buried ionizable side-chain in a protein to be involved in interactions with the backbone / side-chain dipole or oppositely charged side-chain group[70]. The residues Lys 531, Ser 532 and Leu 539 from the two turns of polη-RIR α-helix following the FF sequence interact with Ala 1160, Gly 1161 form the N-terminal β-hairpin of Rev1-CT, while Thr 528 and Glu 529 preceding the FF pair pack against the side-chains of Pro1 182 and Met 1183 in the H1-H2 loop.

The spatial structure of Rev1-CT/polη-RIR complex (Figure 3) reveals that the two consecutive phenylalanine residues, Phe 531 and Phe 532, of the polη RIR motif are responsible for the majority of specific inter-molecular interactions and are crucial for the complex formation. Accordingly, mutation of these critical Phe 531 and Phe 532 residues to glycine within the polη RIR nearly completely eliminates interaction with the Rev1-CT via the yeast two-hybrid system described below (Figure 4A). We also observe a relatively weaker binding when the Phe 483 and Phe 484 residues within the first RIR of polη were mutated to glycine, consistent with an earlier report that all four phenylalanine residues within the two polη RIRs contribute to Rev1-binding[30].

Another important interaction involves the backbone amide groups of Phe 531 and Phe 532 from the N-terminal face of polη-RIR α-helix and negatively charged Asp 1186 of Rev1-CT completely buried on the binding interface. The fact that polη-RIR peptide adopts an α-helical conformation provides a rationale for the previously published mutational data[30]. It is clear that the helix is needed to maintain proper orientation of the two aromatic rings of the FF sequence that fit into the binding pocket on Rev1-CT surface, as well as to position the backbone amides of the first α-helix turn towards the side-chain of Asp 1186 in Rev1-CT. Mutational data suggest that at least four residues following the FF sequence are necessary to maintain α-helical conformation secured by hydrogen bonds between residues *i* and *i*+4. Alanine is highly favorable in α-helices[71], so that substitution of residues C-terminal to the FF sequence with Ala maintains α-helical conformation of RIR peptide and, therefore, has little effect on Rev1-CT binding. In contrast, mutation to a helix-breaking Pro[71] disrupts the α-helix of RIR motif and thereby abolishes Rev1-CT interaction. The α-helix of RIR motifs found in Y-family DNA polymerases starts with the FF sequence following the N-cap Ser or Pro (Figure 1D). Pro is often found in N-cap positions of protein α-helices[72], while Ser is known as one of the most favorable N-cap residues (along with Asn, Asp, Cys and Thr)[73]. Therefore, it is not surprising that Ser to Ala substitution in the polκ-RIR motif results in weakening of Rev1-CT binding[30]. Although, Thr 528 and Glu 529 preceding the FF sequence interact with the side-chain of Met 1183 of Rev1-CT (Figure 3), these and other residues from the N-terminal part of polη-RIR peptide exhibit no well-

defined conformation and are likely of little importance for interaction with Rev1-CT. Therefore, based on our analysis of Rev1-CT/polη-RIR structure (Figure 3) Rev1 binding motif can be re-defined as nFF(4h), where n is an N-cap residue, F is phenylalanine and 4h are at least four residues that form an α-helix.

Corroboration of Rev1-CT/Polη-RIR interface by yeast two-hybrid assays

Having elucidated the structure of the human Rev1 C-terminus in complex with the polη-RIR, we employed a yeast two-hybrid system to monitor the interaction between the proteins. The region encoding the human Rev1-CT and full-length polη was fused to the Activation Domain (AD) and the Binding Domain (BD) of the *GAL4* transcription factor, respectively. The presence of the constructs after transformation into the PJ69-4A strain of yeast was ensured by growth on selective media plates lacking leucine and tryptophan (-LW). Interactions between the two proteins activate the expression of the *HIS3* and *ADE2* reporter genes, both driven by promoters responsive to the Gal4 transcription factor. These interactions were scored by growth on selective media plates additionally lacking adenine and histidine (-AHLW). We determined that a longer Rev1-CT construct of ~120 amino acids, rather than the 95 amino acid Rev1-CT fragment that was used in structure determination, reproducibly recapitulated the interaction with polη. Consistent with earlier data, the interaction between the Rev1-CT and full-length polη resulted in robust growth of the strains in –AHLW selective media plates (Figure 4A). In contrast, no growth was observed in strains expressing the Rev1-CT and the BD alone, showing that the interaction is specific between the two proteins.

Having established a strong interaction between the Rev1-CT and polη we asked if mutations of residues within the N-terminal β-hairpin and α-helices H1, H2 of Rev1-CT affect the interaction with polη. To extend and validate our predictions from the Rev1-CT/polη-RIR complex, we created a series of point mutations within the Rev1-CT and examined its interaction with polη via the yeast two-hybrid assay. As shown in Figure 4B, the Rev1-CT mutations L1159A, L1171A, L1172A, W1175A and D1186A completely abrogate the interaction, whereas the mutations E1174A, T1178A and M1183A severely diminish binding to polη. The mutant proteins containing A1160G, I1179A and Q1189A substitutions, however, show an interaction similar to wild-type Rev1-CT. Among the set of residues in Rev1-CT that show complete loss of binding, Leu 1159 lies on the interface between the N-terminal β-hairpin and helices H1 and H2 that create a binding pocket for the Phe 531 and Phe 532 residues of the polη-RIR, and likely is important for stabilization of the β-hairpin. The key residue Leu 1171 interacts with Phe 532 and is exposed in the free Rev1-CT but becomes buried upon binding the polη-RIR. Its mutation to alanine, therefore, completely eliminates the interaction with the polη-RIR. Leu 1172, however, forms part of the hydrophobic core of the Rev1-CT so a change to alanine, while rendering it incompetent to bind polη, is likely due to a destabilization of the Rev1-CT itself. Similarly Trp 1175, one of the key residues on the binding interface between the Rev1-CT and polη interacts with Phe 532, but is partially buried in the free domain and, therefore, participates in stabilization of the hydrophobic core. Like L1172A, the W1175A mutation likely significantly destabilizes the Rev1-CT domain. Strikingly, Asp 1186, a crucial residue for the Rev1-CT - polη-RIR interaction is almost completely buried on the binding interface. It interacts with the backbone amide groups of Phe 531 and Phe 532 from the first turn of polη-RIR α-helix and, consequently, mutation of this negatively charged amino acid to alanine abrogates interaction with the polη-RIR, as evidenced by a complete lack of growth of yeast strains harboring these plasmids on selective media plates lacking AHLW (Figure 4B).

The weaker polη-RIR interacting residues Glu 1174 and Thr 1178 in the Rev1-CT are located in the α-helix H1 at the periphery of polη-RIR binding interface, while Met 1183 is located in the loop between helices H1 and H2 and interacts with N-terminal residues of the

polη-RIR preceding the conserved Phe 531 and Phe 532. Their mutation to alanine results in a significantly reduced growth of yeast strains carrying the plasmids on –AHLW plates. Surprisingly, mutation of Ala 1160, which makes contacts with the two turns of the polη-RIR α-helix following the FF motif, and Ile 1179, Gln 1189 located on the periphery of the interface and interacting directly with Phe 531 and Phe 532, had no effect on binding to the Rev1-CT in the yeast two-hybrid assay (Figure 4B). Taken together, these results show that the residues Leu 1171, Glu 1174, Thr 1178, Met 1183 and Asp 1186 the Rev1-CT make contacts with polη that contribute to stabilization of the complex between the two proteins.

Conformational dynamics of Rev1-CT domain and Rev1-CT/polη-RIR complex

Protein conformational flexibility plays an important role in molecular recognition, often conferring upon protein domains the ability to bind multiple targets[74,75]. Pre-sampling of multiple interconverting conformers enables rapid selection of molecular configuration optimal for binding. On the other hand, loss of conformational mobility and/or ordering upon binding imposes an entropic penalty that weakens molecular interaction, thereby modulating specificity of recognition by allowing more selective binding. Not surprisingly, a number of molecular complexes have been described involving flexible and/or disordered interaction partner(s) that only fold into an ordered structure upon binding[75]. The interaction between the Rev1-CT and the Y-family DNA polymerases polη, ι, and κ seems to fall into this category. The Rev1 interacting regions (RIRs) of polη, polι, polκ are mapped outside structured domains of the enzymes [5-7] and likely adopt α-helical conformation only upon binding the Rev1-CT domain. Although the Rev1-CT is shown to be well structured, NMR line broadening in H1-H2 and H3-H4 loops, as well as in parts of helices H1 and H2 points to ms-μs conformational rearrangements of RIR interaction interface. Therefore, to elucidate the role of Rev1-CT flexibility in Y-family DNA polymerase recognition we have examined ps-ns and ms- μs time-scale conformational dynamics of free and polη-RIR bound forms of the domain using ^{15}N spin-relaxation[44] and ^{15}N CPMG relaxation dispersion[45] measurements.

Figure 5A (top plots) shows ^{15}N R_1, R_2 relaxation rates and ^{15}N{^{1}H} NOE values for the Rev1-CT domain (red) and Rev1-CT/polη-RIR complex (blue) measured at 11.7 T magnetic field, 15 °C. NMR spin-relaxation data were analyzed using Lipari-Szabo model-free approach[44,56], to extract order parameters S^2 (Figure 5A, bottom plot) and correlation times (data not shown), describing angular amplitudes and time-scales *of fast ps-ns internal motions* of the backbone NH vectors, respectively, along with parameters of overall rotational diffusion of the molecule. As expected, overall rotation correlation time τ_R for the complex (10.45±0.06 ns) exceeds τ_R for the free domain (8.96±0.07 ns) by 17%, closely matching the increase of molecular size upon Rev1-CT (95 aa) - polη -RIR (16 aa) complex formation. Uniformly high order parameters S^2 >0.8 are observed for the backbone amide groups of the free Rev1-CT domain and the complex (Figure 5A), stemming from fast (fs-ps) restricted thermal flexibility of the protein backbone (S^2=1 for fully constrained, 0 for unrestricted motions). The exceptions are 5-6 residues in the C-terminal part of the domain and residues from H3-H4 loop, exhibiting lower S^2 pointing to increased ps-ns mobility. The experimental S^2 (Figure 5A) are in line with those predicted from the backbone chemical shifts using RCI approach[66,67], (Figure 1C), albeit the later are underestimated in loop regions. Interestingly, the experimental S^2 for the backbone amides in the N-terminal β-hairpin are about as high as in the regular secondary structure elements (Figure 5A), confirming that the N-terminal part adopts rigid conformation in both free and bound forms of the Rev1-CT domain. Overall, ^{15}N relaxation data analysis suggests that ps-ns time-scale internal motions of the Rev1-CT domain are restricted and that ps-ns dynamics of the domain does not change upon polη-RIR binding.

Along with order parameters S^2 and correlation times of internal motions, model-free analysis of ^{15}N relaxation data allows extraction of exchange contributions $R_{ex,mf}$ to transverse relaxation rates R_2 that report on *μs-ms conformational dynamics* accompanied by changes in ^{15}N chemical shifts[44]. The extracted $R_{ex,mf}$ primarily originate from faster μs-ms processes, since CPMG sequence in our ^{15}N R_2 experiment suppresses contributions to R_2 due to ms exchange with $k_{ex} \ll 2\pi\nu_{CPMG}$ and $\Delta\omega \ll 2\pi\nu_{CPMG}$ (where k_{ex} is exchange rate constant, $\Delta\omega$ is frequency difference between the exchanging states; CPMG frequency ν_{CPMG} in our ^{15}N R_2 experiment was set to 500 Hz)[58]. To additionally quantify contributions to ^{15}N R_2 rates due to slower ms time-scale conformational exchange, we have performed ^{15}N CPMG relaxation dispersion experiments[45,59,60] that measure effective transverse relaxation rates $R_{2,eff}$ as a function of ν_{CPMG}, and quantified $R_{ex,rd} = R_{2,eff}^{clc}(33Hz)-R_{2,eff}^{clc}(533Hz)$ that complement $R_{ex,mf}$ obtained in model-free analysis of ^{15}N relaxation data. The sum $R_{ex,mf}+R_{ex,rd}$ provides an approximation for total exchange contribution R_{ex} to ^{15}N R_2 in free-precession limit.

^{15}N R_2 rates plotted *vs.* residue number (Figure 5A) reveal that residues in (and adjacent to) H1-H2 and H3-H4 loops in the free Rev1-CT domain and in the complex exhibit enhanced ^{15}N R_2 caused by significant μs-ms exchange contributions $R_{ex,mf}$ that were quantified using model-free analysis of ^{15}N spin-relaxation data[44,56]. ^{15}N CPMG relaxation dispersion measurements[45,59,60] that were used to identify amide groups involved in slower ms time-scale exchange not captured in $R_{ex,mf}$ significantly extend the list of residues in free and bound forms of Rev1-CT undergoing μs-ms conformational rearrangements. Figure 5B shows examples of ^{15}N CPMG relaxation dispersion profiles for the backbone amide groups of Gly 1161, Leu 1171, Trp 1175 and Asp 1186 that form polη) binding site of Rev1-CT. In is clear that for these residues $R_{2,eff}(\nu_{CPMG})$ profiles reach a plateau at ν_{CPMG}~500 Hz where the exchange contribution to R_2 is effectively suppressed by CPMG sequence. Figure 5C shows total exchange contribution $R_{ex} = R_{ex,mf}+R_{ex,rd}$ to ^{15}N R_2 rates (at 11.7 T magnetic field) mapped onto structures of free Rev1-CT domain (top) and the complex (bottom), with residues involved in faster μs-ms and slower ms dynamics marked, respectively, in cyan and magenta. Remarkably, the region exhibiting extensive μs-ms conformational exchange in both free and bound states of Rev1-CT encompasses the binding site for the polη -RIR motif formed by residues from the N-terminal β-hairpin, the two last turns of α-helix H1, the H1-H2 loop, and two first turns of α -helix H2. Although μs-ms exchange contributions R_{ex} generally decrease upon the complex formation, the binding interface remains dynamic on μs-ms time-scale in Rev1-CT/polη-RIR complex. Interestingly, R_{ex} contribution to ^{15}N R_2 increase upon the complex formation for Gly 1161 from the N-terminal β-hairpin of Rev1-CT (Figure 5B), which directly interacts with polη-RIR α-helix.

Beyond intramolecular processes, ms time-scale exchange observed in the Rev1-CT/polη RIR complex may be caused by an on-off equilibrium between free and bound forms of the protein[76].From the upper limits of k_{on} (2.7×10^6 M^{-1} s^{-1}) and k_{off} (33 s^{-1}) obtained as described above one can derive the upper estimate for the exchange rate constant of the on-off equilibrium $k_{ex} = k_{on}[L]+k_{off}$ ~ 300 s^{-1} at the condition of our ^{15}N CPMG dispersion experiment (0.9 mM total protein, 0.9 mM total peptide concentrations; free ligand concentration [L] ~ 11% of 0.9 mM at K_D = 13 μM[30]). Even at a relatively slow k_{ex} of 100-300 s^{-1} the exchange between free and bound forms of Rev1-CT may cause noticeable exchange contributions to transverse relaxation rates. To elucidate whether the observed ms time-scale exchange in the complex can be solely explained by on-off equilibrium between free and bound forms of Rev1-CT we have additionally recorded ^{15}N CPMG dispersion profiles at 18.8 T magnetic field, and globally fit 11.7 and 18.8 T relaxation dispersion data to a model of two-state conformational exchange (see supplementary Figure 2S), resulting in a population of the second (minor) state p_B = 5.9±0.4% and exchange rate constant k_{ex} =

585±23 s^{-1}. This is about two times faster than the estimated 300 s^{-1} upper limit of the exchange rate constant for the Rev1-CT/polη -RIR binding equilibrium. Interestingly, ^{15}N chemical shift differences obtained from CPMG relaxation dispersion data, $\Delta\omega_{disp}$, are in good agreement with ^{15}N chemical shift differences between free and polη-RIR bound forms of Rev1-CT, $\Delta\omega_{spec}$ (supplementary Figure 2S), with the exception of few residues on the binding interface (such as Trp 1175). In addition, significant contributions $R_{ex,mf}$ to ^{15}N transverse relaxation rates R_2 due to faster |j,s-ms dynamics have been obtained in 'model-free' analysis of ^{15}N relaxation data for the binding site residues 1175-1179 (Figure 5A,C). Taken together, these data suggest that conformational exchange observed on the binding interface of the Rev1-CT -polη -RIR complex may include contributions from both on-off equilibrium between free and bound forms of Rev1-CT and intra-molecular dynamic process(es).

The analysis of ^{15}N spin-relaxation and ^{15}N CPMG relaxation dispersion data established that that free and polη-RIR bound forms of Rev1-CT domain are rigid on ps-ns time scale, but exhibit significant μs-ms conformational dynamics encompassing the RIR binding site. Transitions to low-populated states occurring on μs-ms time-scale observed on intermolecular interface of the complex may point to the existence of multiple modes of Rev1-CT/polη-RIR binding. Such a plasticity of interaction interface in the bound state might prove beneficial for minimizing entropic penalty of the complex formation[75]. On the other hand, μs-ms sampling of multiple conformational states in free Rev1-CT domain may facilitate selection of molecular configuration(s) that enable efficient binding of RIR motifs[74,75], exhibiting surprisingly little sequence conservation among Y-family DNA polymerases (Figure 1D).

Concluding Remarks

In this study, we have made a significant contribution to our understanding of how Rev1 regulates TLS in human cells through its interactions with the Y-family TLS polymerases polη, ι and κ by (i) solving the structure of Rev1's important C-terminal domain, (ii) revealing the structural details of how the RIR of polη binds to Rev1's C-terminal domain, and (iii) showing that the RIR binding site of the Rev1 C-terminal domain displays conformational dynamics on the μs-ms time scale that may facilitate the selection of the molecular configuration optimal for binding. We have also been able to redefine the Rev1 binding motif, RIR, as nFF(4h), where n is an N-cap residue, F is phenylalanine and 4h are at least four residues that form an α-helix.

The interactions that Rev1 makes with the Y-family DNA polymerases polη, ι, and κ enable a later acting form of TLS control that acts subsequent to the Rad6/Rad18-mediated monoubiquitination of PCNA that is triggered by a variety of types of DNA damage[12,77]. The Rev1-CT is not important for the recognition of monoubiquitinated PCNA nor is it necessary for recruitment to nuclear foci after DNA damage[64,78]. Reciprocally, the RIR sequences of polη are not necessary for recruitment to UV-induced nuclear foci, since its C-terminal 120 amino acids which do not include either of the RIRs are sufficient for its localization[79]. Nor are the RIR sequences necessary for damage-induced foci formation by polκ[30] or polι[80]. Thus the interactions that the Y-family TLS DNA polymerases polη, ι, and κ make with the Rev1-CT represent another level of regulation beyond that of PCNA monoubiqutination that helps to ensure that these inherently error-prone DNA polymerases do not introduce mutations by gaining access to primer termini in undamaged DNA. Subsequent polymerase exchanges that are mediated through the interactions that each of these TLS polymerases make with Rev1's C-terminal domain could possibly also help with the process of matching each polymerase with its cognate lesion over which it can replicate relatively accurately. Example of cognate lesions include thymine-thymine cyclobutane

pyrimidine dimers for polη, N^2-BPDE-dG lesions for polκ, and εdA for polι[1,5]. Polymerase exchange mediated by the Rev1 C-terminal domain could also help exchange a non functional TLS polymerase for an alternative TLS polymerase[81]. Evidence has been reported indicating that, in higher eukaryotes, a component of TLS can also proceed in the absence of PCNA monoubiquitination[82]. In these cases, the interactions that Rev1 makes with other TLS DNA polymerases might be particularly important in facilitating and regulating TLS[37,39,83]. The exchanges that Rev1 likely facilitates between polη, ι and κ are apparently made possible by the μs-ms conformational dynamics of the region of the Rev1-CT that interacts with their RIRs.

In TLS events requiring the coordinated consecutive action of two DNA polymerases, the Rev1 C-terminal domain can also serve to facilitate the exchange from an inserter DNA polymerase to the extender DNA polymerase polζ via its interaction with the accessory subunit Rev7. Recent evidence indicates that human Rev1 recruits polζ through an interaction with Rev7 as it does in yeast[84]. Rev7 clearly interacts differently with the Rev1-CT than do polη, ι, and κ since it lacks an RIR and the Rev1-binding interface of Rev7 appears be a portion of the surface of a five-stranded β-sheet of Rev7 rather than a disordered peptide[85]. Although polη can accurately replicate UV-irradiated DNA independently of Rev1, polη -Rev1 interactions are involved in suppressing spontaneous mutations, probably by promoting accurate TLS past endogenous lesions[86].

Although TLS DNA polymerases can act at the replication fork, there is a growing body of evidence in both yeast and mammalian cells that a substantial amount of TLS occurs at postreplicational gaps caused by lesions rather than at active replication forks[8-12,87]. In fact, in yeast TLS occurs efficiently if it is constrained to occur during G2/M by manipulating the cell cycle dependence of Rad6/Rad18-dependent monoubiquitination[8,10]. Of particular interest is the observation that in *S. cerevisiae* Rev1 is synthesized at extremely low levels during G1 and most of S phase, but then is expressed at fifty fold higher levels during G2/M[87]. Thus, most of the Rev1-polζ interaction that occur in *S. cerevisae* via interactions of the Rev1 C-terminal domain with Rev7 are naturally confined to postreplicational gaps during G2/M[11,88]. Given the growing body of evidence that a significant amount of TLS takes place during G2/M in mammalian cells[9], it seems likely that a substantial fraction of the interactions between the Rev1 C-terminal domain and other TLS DNA polymerases similarly take place at postreplicational gaps.

Knowledge of the structure of the Rev1-CT should also make it possible to clarify the molecular details of the interactions that Rev1 makes during interstrand crosslink repair and may make it possible to gain additional insights into the relationship between interstrand crosslink repair and Fanconi anemia[89]. Since inhibition of TLS can help to improve chemotherapy[90,91], it is possible that searching for inhibitors that target specific protein-protein interactions required for TLS might be an alternative to searching for inhibitors that selectively inhibit only one TLS DNA polymerase out of the 15 DNA polymerases found in human cells[92].

Supplementary Material

Refer to Web version on PubMed Central for supplementary material.

Acknowledgments

This work was supported by a grant from the NIH (P30GM092369) and UCHC startup funds to D.M.K.; S.D. and G.C.W. are supported by NIEHS ES015818 and grant P30 ES002109 from the Center of Environmental Health Sciences (MIT). G.C.W. is an American Cancer Society Research Professor.

References

1. Friedberg, EC.; Walker, GC.; Siede, W.; Wood, RD.; Schultz, RA.; Ellenberger, T. DNA Repair and Mutagenesis. Second. ASM Press; Washington, D. C: 2005.
2. Goodman MF. Error-prone repair DNA polymerases in prokaryotes and eukaryotes. Annu Rev Biochem. 2002; 71:17–50. [PubMed: 12045089]
3. Prakash S, Johnson RE, Prakash L. Eukaryotic translesion synthesis DNA polymerases: specificity of structure and function. Annu Rev Biochem. 2005; 74:317–353. [PubMed: 15952890]
4. Lehmann AR, Niimi A, Ogi T, Brown S, Sabbioneda S, Wing JF, Kannouche PL, Green CM. Translesion synthesis: Y-farnily polymerases and the polymerase switch. DNA Repair. 2007; 6:891–899. [PubMed: 17363342]
5. Waters LS, Minesinger BK, Wiltrout ME, D'Souza S, Woodruff RV, Walker GC. Eukaryotic translesion polymerases and their roles and regulation in DNA damage tolerance. Microbiol Mol Biol Rev. 2009; 73:134–154. [PubMed: 19258535]
6. Guo CX, Kosarek-Stancel J, Tang TS, Friedberg EC. Y-family DNA polymerases in mammalian cells. Cell Mol Life Sci. 2009; 66:2363–2381. [PubMed: 19367366]
7. Sale JE, Lehmann AR, Woodgate R. Y-family DNA polymerases and their role in tolerance of cellular DNA damage. Nat Rev Mol Cell Biol. 2012; 13:141–152. [PubMed: 22358330]
8. Daigaku Y, Davies AA, Ulrich HD. Ubiquitin-dependent DNA damage bypass is separable from genome replication. Nature. 2010; 465:951–955. [PubMed: 20453836]
9. Diamant N, Hendel A, Vered I, Carell T, Reissner T, de Wind N, Geacinov N, Livneh Z. DNA damage bypass operates in the S and G2 phases of the cell cycle and exhibits differential mutagenicity. Nucleic Acids Res. 2012; 40:170–180. [PubMed: 21908406]
10. Karras GI, Jentsch S. The RAD6 DNA damage tolerance pathway operates uncoupled from the replication fork and is functional beyond S phase. Cell. 2010; 141:255–267. [PubMed: 20403322]
11. Lopes M, Foiani M, Sogo JM. Multiple mechanisms control chromosome integrity after replication fork uncoupling and restart at irreparable UV lesions. Mol Cell. 2006; 21:15–27. [PubMed: 16387650]
12. Ulrich HD. Timing and spacing of ubiquitin-dependent DNA damage bypass. FEBS Lett. 2011; 585:2861–2867. [PubMed: 21605556]
13. Yang W. Portraits of a Y-family DNA polymerase. FEBS Lett. 2005; 579:868–872. [PubMed: 15680965]
14. Kunkel TA. DNA replication fidelity. J Biol Chem. 2004; 279:16895–16898. [PubMed: 14988392]
15. Johnson RE, Prakash S, Prakash L. Efficient bypass of a thymine-thymine- dimer by yeast DNA polymerase Polη. Science. 1999; 283:1001–1004. [PubMed: 9974380]
16. Masutani C, Araki M, Yamada A, Kusumoto R, Nogimori T, Maekawa T, Iwai S, Hanaoka F. Xeroderma pigmentosum variant (XP-V) correcting protein from HeLa cells has a thymine dimer bypass DNA polymerase activity. EMBO J. 1999; 18:3491–3501. [PubMed: 10369688]
17. Avkin S, Goldsmith M, Velasco-Miguel S, Geacintov N, Friedberg EC, Livneh Z. Quantitative analysis of translesion DNA synthesis across a benzo[a]pyrene-guanine adduct in mammalian cells: the role of DNA polymerase kappa. J Biol Chem. 2004; 279:53298–53305. [PubMed: 15475561]
18. Jarosz DF, Godoy VG, Delaney JC, Essigmann JM, Walker GC. A single amino acid governs enhanced activity of DinB DNA polymerases on damaged templates. Nature. 2006; 439:225–228. [PubMed: 16407906]
19. Friedberg EC, Lehmann AR, Fuchs RPP. Trading places: How do DNA polymerases switch during translesion DNA synthesis? Mol Cell. 2005; 18:499–505. [PubMed: 15916957]
20. Livneh Z, Ziv O, Shachar S. Multiple two-polymerase mechanisms in mammalian translesion DNA synthesis. Cell Cycle. 2010; 9:729–735. [PubMed: 20139724]
21. Shachar S, Ziv O, Avkin S, Adar S, Wittschieben J, Reissner T, Chaney S, Friedberg EC, Wang ZG, Carell T, Geacintov N, Livneh Z. Two-polymerase mechanisms dictate error-free and error-prone translesion DNA synthesis in mammals. EMBO J. 2009; 28:383–393. [PubMed: 19153606]
22. Lawrence CW. Cellular roles of DNA polymerase zeta and Rev1 protein. DNA Repair (Amst). 2002; 1:425–435. [PubMed: 12509231]

23. Lawrence CW. Cellular functions of DNA polymerase zeta and Rev1 protein. Adv Protein Chem. 2004; 69:167–203. [PubMed: 15588843]
24. Wang Y, Woodgate R, McManus TP, Mead S, McCormick JJ, Maher VM. Evidence that in xeroderma pigmentosum variant cells, which lack DNA polymerase eta, DNA polymerase iota causes the very high frequency and unique spectrum of UV-induced mutations. Cancer Res. 2007; 67:3018–3026. [PubMed: 17409408]
25. Bienko M, Green CM, Crosetto N, Rudolf F, Zapart G, Coull B, Kannouche P, Wider G, Peter M, Lehmann AR, Hofmann K, Dikic I. Ubiquitin- binding domains in Y-family polymerases regulate translesion synthesis. Science. 2005; 310:1821–1824. [PubMed: 16357261]
26. Hoege C, Pfander B, Moldovan GL, Pyrowolakis G, Jentsch S. RAD6-dependent DNA repair is linked to modification of PCNA by ubiquitin and SUMO. Nature. 2002; 419:135–141. [PubMed: 12226657]
27. Guo C, Sonoda E, Tang TS, Parker JL, Bielen AB, Takeda S, Ulrich HD, Friedberg EC. REV1 protein interacts with PCNA: significance of the REV1 BRCT domain in vitro and in vivo. Mol Cell. 2006; 23:265–271. [PubMed: 16857592]
28. Sharma NM, Kochenova OV, Shcherbakova PV. The non-canonical protein binding site at the monomer-monomer interface of yeast proliferating cell nuclear antigen (PCNA) regulates the Rev1-PCNA interaction and Polζ/Rev1-dependent translesion DNA synthesis. J Biol Chem. 2011; 286:33557–33566. [PubMed: 21799021]
29. Wood A, Garg P, Burgers PM. A ubiquitin-binding motif in the translesion DNA polymerase Rev1 mediates its essential functional interaction with ubiquitinated proliferating cell nuclear antigen in response to DNA damage. J Biol Chem. 2007; 282:20256–20263. [PubMed: 17517887]
30. Ohashi E, Hanafusa T, Kamei K, Song I, Tomida J, Hashimoto H, Vaziri C, Ohmori H. Identification of a novel REV1-interacting motif necessary for DNA polymerase kappa function. Genes Cells. 2009; 14:101–111. [PubMed: 19170759]
31. Gibbs PE, Wang XD, Li Z, McManus TP, McGregor WG, Lawrence CW, Maher VM. The function of the human homolog of Saccharomyces cerevisiae REV1 is required for mutagenesis induced by UV light. Proc Natl Acad Sci U S A. 2000; 97:4186–4191. [PubMed: 10760286]
32. Lawrence CW, Maher VM. Mutagenesis in eukaryotes dependent on DNA polymerase zeta and Rev1p. Philos Trans R Soc Lond B Biol Sci. 2001; 356:41–46. [PubMed: 11205328]
33. Masuda Y, Takahashi M, Tsunekuni N, Minami T, Sumii M, Miyagawa K, Kamiya K. Deoxycytidyl transferase activity of the human REV1 protein is closely associated with the conserved polymerase domain. J Biol Chem. 2001; 276:15051–15058. [PubMed: 11278384]
34. Haracska L, Prakash S, Prakash L. Yeast Rev1 protein is a G template-specific DNA polymerase. J Biol Chem. 2002; 277:15546–15551. [PubMed: 11850424]
35. Nelson JR, Lawrence CW, Hinkle DC. Deoxycytidyl transferase activity of yeast REV1 protein. Nature. 1996; 382:729–731. [PubMed: 8751446]
36. Nelson JR, Gibbs PE, Nowicka AM, Hinkle DC, Lawrence CW. Evidence for a second function for Saccharomyces cerevisiae Rev1p. Mol Microbiol. 2000; 37:549–554. [PubMed: 10931348]
37. Guo C, Fischhaber PL, Luk-Paszyc MJ, Masuda Y, Zhou J, Kamiya K, Kisker C, Friedberg EC. Mouse Rev1 protein interacts with multiple DNA polymerases involved in translesion DNA synthesis. EMBO J. 2003; 22:6621–6630. [PubMed: 14657033]
38. Ohashi E, Murakumo Y, Kanjo N, Akagi J, Masutani C, Hanaoka F, Ohmori H. Interaction of hREV1 with three human Y-family DNA polymerases. Genes Cells. 2004; 9:523–531. [PubMed: 15189446]
39. Tissier A, Kannouche P, Reck MP, Lehmann AR, Fuchs RP, Cordonnier A. Co-localization in replication foci and interaction of human Y-family members, DNA polymerase pol eta and REV1 protein. DNA Repair (Amst). 2004; 3:1503–1514. [PubMed: 15380106]
40. Sharma S, Hicks JK, Chute CL, Brennan JR, Ahn JY, Glover TW, Canman CE. REV1 and polymerase zeta facilitate homologous recombination repair. Nucleic Acids Res. 2012; 40:682–691. [PubMed: 21926160]
41. D'Souza S, Waters LS, Walker GC. Novel conserved motifs in Rev1 C-terminus are required for mutagenic DNA damage tolerance. DNA Repair (Amst). 2008; 7:1455–1470. [PubMed: 18603483]

42. Nair DT, Johnson RE, Prakash L, Prakash S, Aggarwal AK. Rev1 employs a novel mechanism of DNA synthesis using a protein template. Science. 2005; 309:2219–2222. [PubMed: 16195463]
43. Swan MK, Johnson RE, Prakash L, Prakash S, Aggarwal AK. Structure of the human Rev1-DNA-dNTP ternary complex. J Mol Biol. 2009; 390:699–709. [PubMed: 19464298]
44. Korzhnev DM, Billeter M, Arseniev AS, Orekhov VY. NMR studies of Brownian tumbling and internal motions in proteins. Prog Nucl Magn Reson Spectrosc. 2001; 38:197–266.
45. Palmer AG, Kroenke CD, Loria JP. Nuclear magnetic resonance methods for quantifying microsecond-to-millisecond motions in biological macromolecules. Methods Enzymol. 2001; 339:204–238. [PubMed: 11462813]
46. Sattler M, Schleucher J, Griesinger C. Heteronuclear multidimensional NMR experiments for the structure determination of proteins in solution employing pulsed field gradients. Prog Nucl Magn Reson Spectrosc. 1999; 34:93–158.
47. Zwahlen C, Legault P, Vincent SJF, Greenblatt J, Konrat R, Kay LE. Methods for measurement of intermolecular NOEs by multinuclear NMR spectroscopy: Application to a bacteriophage lambda N-peptide/boxB RNA complex. J Am Chem Soc. 1997; 119:6711–6721.
48. Delaglio F, Grzesiek S, Vuister GW, Zhu G, Pfeifer J, Bax A. NMRPIPE - a multidimensional spectral processing system based on UNIX pipes. J Biomol NMR. 1995; 6:277–293. [PubMed: 8520220]
49. Keller, RLJ. The computer aided resonance assignment tutorial. Cantina: 2004.
50. Guntert P. Automated NMR protein structure calculation. Prog Nucl Magn Reson Spectrosc. 2003; 43:105–125.
51. Shen Y, Delaglio F, Cornilescu G, Bax A. TALOS plus: a hybrid method for predicting protein backbone torsion angles from NMR chemical shifts. J Biomol NMR. 2009; 44:213–223. [PubMed: 19548092]
52. Brunger AT, Adams PD, Clore GM, DeLano WL, Gros P, Grosse-Kunstleve RW, Jiang JS, Kuszewski J, Nilges M, Pannu NS, Read RJ, Rice LM, Simonson T, Warren GL. Crystallography & NMR system: A new software suite for macromolecular structure determination. Acta Crystallogr Sect D. 1998; 54:905–921. [PubMed: 9757107]
53. Farrow NA, Muhandiram R, Singer AU, Pascal SM, Kay CM, Gish G, Shoelson SE, Pawson T, Formankay JD, Kay LE. Backbone dynamics of a free and a phosphopeptide complexed Src homology-2 domain studied by ^{15}N NMR relaxation. Biochemistry. 1994; 33:5984–6003. [PubMed: 7514039]
54. Korzhnev DM, Tischenko EV, Arseniev AS. Off-resonance effects in ^{15}N T_2 CPMG measurements. J Biomol NMR. 2000; 17:231–237. [PubMed: 10959630]
55. Orekhov VY, Nolde DE, Golovanov AP, Korzhnev DM, Arseniev AS. Processing of heteronuclear NMR relaxation data with the new software DASHA. Appl Magn Reson. 1995; 9:581–588.
56. Lipari G, Szabo A. Model-free approach to theinterpretation of nuclear magnetic resonance relaxation in macromolecules.1.Theory and range of validity. J Am Chem Soc. 1982; 104:4546–4559.
57. Mandel AM, Akke M, Palmer AG. Backbone dynamics of *Escherichia coli* ribonuclease HI: correlations with structure and function in an active enzyme. J Mol Biol. 1995; 246:144–163. [PubMed: 7531772]
58. Ishima R, Torchia DA. Estimating the time scale of chemical exchange of proteins from measurements of transverse relaxation rates in solution. J Biomol NMR. 1999; 14:369–372. [PubMed: 10526408]
59. Loria JP, Rance M, Palmer AG. A relaxation-compensated Carr-Purcell-Meiboom-Gill sequence for characterizing chemical exchange by NMR spectroscopy. J Am Chem Soc. 1999; 121:2331–2332.
60. Hansen DF, Vallurupalli P, Kay LE. An improved ^{15}N relaxation dispersion experiment for the measurement of millisecond time-scale dynamics in proteins. J Phys Chem B. 2008; 112:5898–5904. [PubMed: 18001083]
61. Korzhnev DM, Salvatella X, Vendruscolo M, Di Nardo AA, Davidson AR, Dobson CM, Kay LE. Low-populated folding intermediates of Fyn SH3 characterized by relaxation dispersion NMR. Nature. 2004; 430:586–590. [PubMed: 15282609]

62. James P, Halladay J, Craig EA. Genomic libraries and a host strain designed for highly efficient two-hybrid selection in yeast. Genetics. 1996; 144:1425–1436. [PubMed: 8978031]
63. Guo D, Xie Z, Shen H, Zhao B, Wang Z. Translesion synthesis of acetylaminofluorene-dG adducts by DNA polymerase zeta is stimulated by yeast Rev1 protein. Nucleic Acids Res. 2004; 32:1122–1130. [PubMed: 14960722]
64. Ross AL, Simpson LJ, Sale JE. Vertebrate DNA damage tolerance requires the C-terminus but not BRCT or transferase domains of REV1. Nucleic Acids Res. 2005; 33:1280–1289. [PubMed: 15741181]
65. Kosarek JN, Woodruff RV, Rivera-Begeman A, Guo CX, D'Souza S, Koonin EV, Walker GC, Friedberg EC. Comparative analysis of in vivo interactions between Rev1 protein and other Y-family DNA polymerases in animals and yeasts. DNA Repair. 2008; 7:439–451. [PubMed: 18242152]
66. Berjanskii MV, Wishart DS. A simple method to predict protein flexibility using secondary chemical shifts. J Am Chem Soc. 2005; 127:14970–14971. [PubMed: 16248604]
67. Berjanskii MV, Wishart DS. Application of the random coil index to studying protein flexibility. J Biomol NMR. 2008; 40:31–48. [PubMed: 17985196]
68. Bain AD. Chemical exchange in NMR. Prog Nucl Magn Reson Spectrosc. 2003; 43:63–103.
69. Schreiber G. Kinetic studies of protein-protein interactions. Curr Opin Struct Biol. 2002; 12:41–47. [PubMed: 11839488]
70. Kim J, Mao J, Gunner MR. Are acidic and basic groups in buried proteins predicted to be ionized? J Mol Biol. 2005; 348:1283–1298. [PubMed: 15854661]
71. Chakrabartty A, Baldwin RL. Stability of alpha-helices. Adv Protein Chem. 1995; 46:141–176. [PubMed: 7771317]
72. Viguera AR, Serrano L. Stable proline box motif at the N-terminal end of alpha-helices. Protein Sci. 1999; 8:1733–1742. [PubMed: 10493574]
73. Doig AJ, Baldwin RL. N- and C-capping preferences for all 20 amino-acids in alpha-helical peptides. Protein Sci. 1995; 4:1325–1336. [PubMed: 7670375]
74. Boehr DD, Nussinov R, Wright PE. The role of dynamic conformational ensembles in biomolecular recognition. Nat Chem Biol. 2009; 5:789–796. [PubMed: 19841628]
75. Mittag T, Kay LE, Forman-Kay JD. Protein dynamics and conformational disorder in molecular recognition. J Mol Recognit. 2010; 23:105–116. [PubMed: 19585546]
76. Sugase K, Lansing JC, Dyson HJ, Wright PE. Tailoring relaxation dispersion experiments for fast-associating protein complexes. J Am Chem Soc. 2007; 129:13406–13407. [PubMed: 17935336]
77. Zhang W, Qin Z, Zhang X, Xiao W. Roles of sequential ubiquitination of PCNA in DNA-damage tolerance. FEBS Lett. 2011; 585:2786–2794. [PubMed: 21536034]
78. Guo C, Tang TS, Bienko M, Parker JL, Bielen AB, Sonoda E, Takeda S, Ulrich HD, Dikic I, Friedberg EC. Ubiquitin-binding motifs in REV1 protein are required for its role in the tolerance of DNA damage. Mol Cell Biol. 2006; 26:8892–8900. [PubMed: 16982685]
79. Kannouche P, Broughton BC, Volker M, Hanaoka F, Mullenders LH, Lehmann AR. Domain structure, localization, and function of DNA polymeraseeta, defective in xeroderma pigmentosum variant cells. Genes Dev. 2001; 15:158–172. [PubMed: 11157773]
80. Vidal AE, Kannouche P, Podust VN, Yang W, Lehmann AR, Woodgate R. Proliferating cell nuclear antigen-dependent coordination of the biological functions of human DNA polymerase iota. J Biol Chem. 2004; 279:48360–48368. [PubMed: 15342632]
81. Ito W, Yokoi M, Sakayoshi N, Sakurai Y, Akagi JI, Mitani H, Hanaoka F. Stalled Poleta at its cognate substrate initiates an alternative translesion synthesis pathway via interaction with REV1. Genes Cells. 2012
82. Edmunds CE, Simpson LJ, Sale JE. PCNA ubiquitination and REV1 define temporally distinct mechanisms for controlling translesion synthesis in the avian cell line DT40. Mol Cell. 2008; 30:519–529. [PubMed: 18498753]
83. Murakumo Y, Ogura Y, Ishii H, Numata S, Ichihara M, Croce CM, Fishel R, Takahashi M. Interactions in the error-prone postreplication repair proteins hREV1, hREV3, and hREV7. J Biol Chem. 2001; 276:35644–35651. [PubMed: 11485998]

84. Hashimoto K, Cho Y, Yang IY, Akagi J, Ohashi E, Tateishi S, de Wind N, Hanaoka F, Ohmori H, Moriya M. The vital role of polymerase zeta and REV1 in mutagenic, but not correct, DNA synthesis across benzo[a]pyrene-dG and recruitment of polymerase zeta by REV1 to replication-stalled site. J Biol Chem. 2012; 287:9613–9622. [PubMed: 22303021]

85. Hara K, Hashimoto H, Murakumo Y, Kobayashi S, Kogame T, Unzai S, Akashi S, Takeda S, Shimizu T, Sato M. Crystal structure of human REV7 in complex with a human REV3 fragment and structural implication of the interaction between DNA polymerase zeta and REV1. J Biol Chem. 2010; 285:12299–12307. [PubMed: 20164194]

86. Akagi J, Masutani C, Kataoka Y, Kan T, Ohashi E, Mori T, Ohmori H, Hanaoka F. Interaction with DNA polymerase eta is required for nuclear accumulation of REV1 and suppression of spontaneous mutations in human cells. DNA Repair (Amst). 2009; 8:585–599. [PubMed: 19157994]

87. Waters LS, Walker GC. The critical mutagenic translesion DNA polymerase Rev1 is highly expressed during G(2)/M phase rather than S phase. Proc Natl Acad Sci U S A. 2006; 103:8971–8976. [PubMed: 16751278]

88. D'Souza S, Walker GC. Novel role for the C terminus of Saccharomyces cerevisiae Rev1 in mediating protein-protein interactions. Mol Cell Biol. 2006; 26:8173–8182. [PubMed: 16923957]

89. Kim H, Yang KL, Dejsuphong D, D'Andrea AD. Regulation of Rev1 by the Fanconi anemia core complex. Nat Struct Mol Biol. 2012; 19:164–170. [PubMed: 22266823]

90. Doles J, Oliver TG, Cameron ER, Hsu G, Jacks T, Walker GC, Hemann MT. Suppression of Rev3, the catalytic subunit of Polζ, sensitizes drug-resistant lung tumors to chemotherapy. Proc Natl Acad Sci U S A. 2010; 107:20786–20791. [PubMed: 21068376]

91. Xie K, Doles J, Hemann MT, Walker GC. Error-prone translesion synthesis mediates acquired chemoresistance. Proc Natl Acad Sci U S A. 2010; 107:20792–20797. [PubMed: 21068378]

92. Lange SS, Takata K, Wood RD. DNA polymerases and cancer. Nat Rev Cancer. 2011; 11:96–110. [PubMed: 21258395]

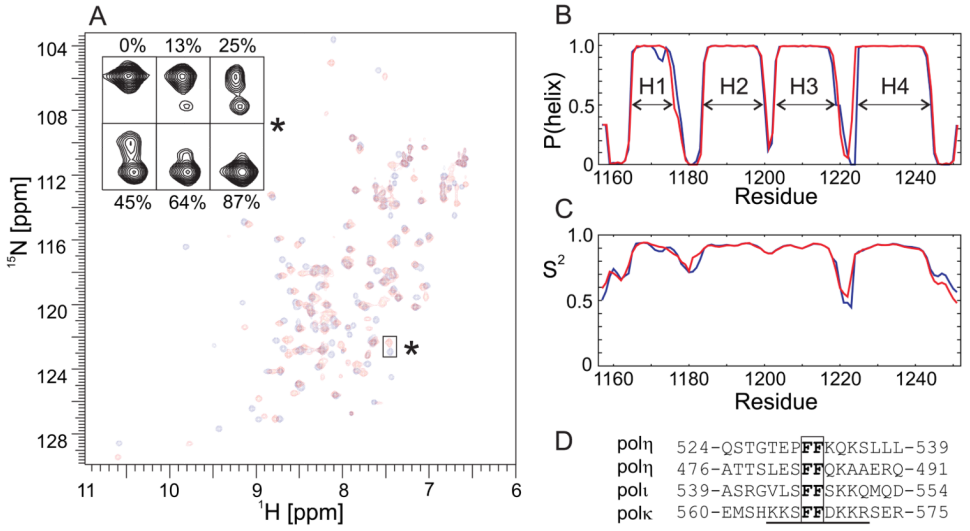

Figure 1.

(**A**) ^{1}H-^{15}N HSQC spectra of free ^{15}N/^{13}C Rev 1-CT domain (red) and ^{15}N/^{13}C Rev1-CT complex with unlabeled polη -RIR peptide (blue) recorded at 11.7 T magnetic field, 15 °C. Inset shows the peak of Leu 1171 in ^{1}H-^{15}N HSQC spectra of a titration series recorded at different ratios of peptide to protein. (**B**) Probability of α-helix, P(helix), in free (red) and polη-RIR bound (blue) Rev1-CT domain predicted from the backbone chemical shifts using TALOS+ program[51] plotted *vs.* residue number. (**C**) Order parameters S^2 for the backbone amide groups of free (red) and polη-RIR bound (blue) Rev1-CT domain predicted from the backbone chemical shifts using RCI approach[66,67]. (**D**) Alignment of 16 aa peptides comprising RIR regions of human polη, ι κ used by Ohashi et al.[30] to identify minimal motif required for Rev1-CT interaction (underlined). The two consecutive Phe residues shown in the box are the only residues conserved in all four RIR regions found in human Y-type DNA polymerases.

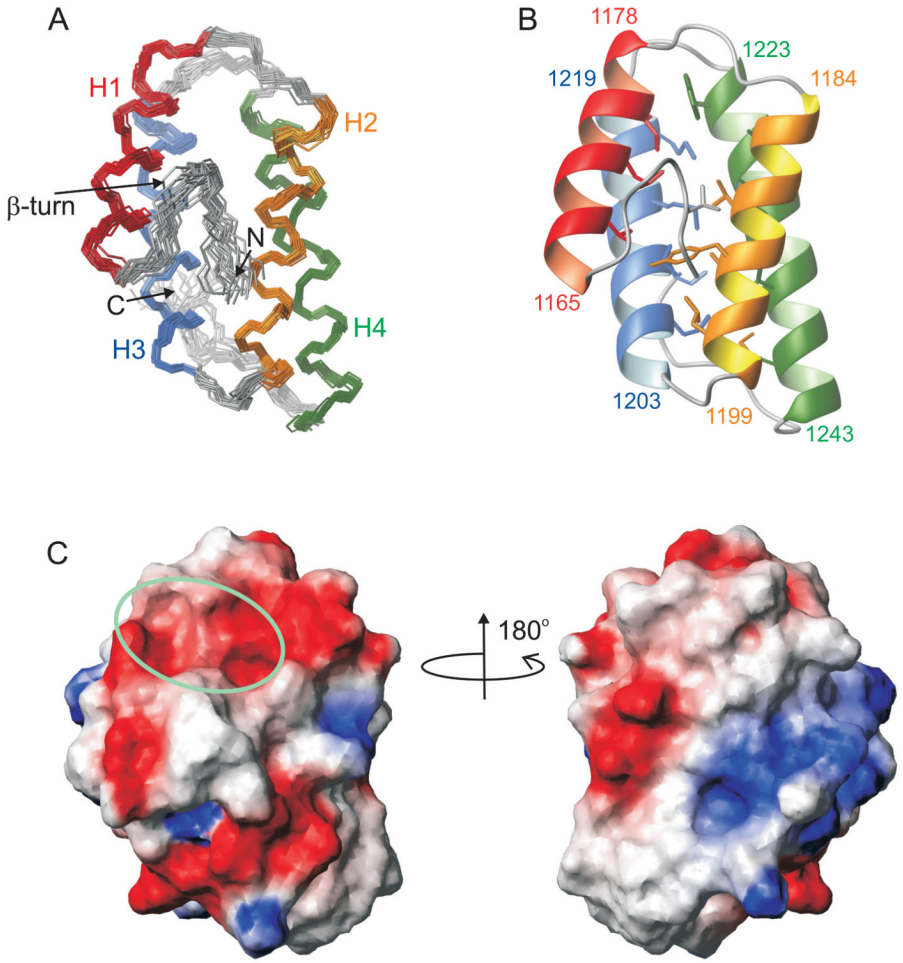

Figure 2.

Three-dimensional structure of human Rev1-CT domain (residues 1157-1251) determined by solution NMR spectroscopy. (**A**) Superposition of the backbone folds of 20 final lowest-energy structures obtained in CYANA[50] followed by refinement in explicit solvent by CNS software[52]. (**B**) Ribbon representation of Rev1-CT structure showing the positions of four α-helixes of the domain. Side chains are shown for residues that form core of the domain with less than 10% surface exposure and 10 Å^2 accessible surface area (averaged over 20 best structures), including Leu 1159, Ala 1162 from the N-terminal β-hairpin, Val 1168, Leu 1172 (*rev1-108*), Ile 1176 (*rev1-108*) from α-helix H1, Val 1190 (*rev1-110*), Tyr 1193 (*rev1-110*), Cys 1194 (*rev1-110*), Leu 1197, Ile 1198 from α-helix H2, Leu 1206 (*rev1-111*), Val 1209 (*rev1-111*), Ile 1210 (*rev1-111*), Met 1213, Leu 1216, Met 1217 from α-helix H3, Trp 1225, Ala 1228, Ile 1232, Val 1236, Leu 1240 from α-helix H4; underlined are residues from four conserved 5-6 aa residue regions, referred to as *rev1-108* to *-111*, identified by extensive sequence alignment of Rev1-CT domains from different eukaryotic species[41]. (**C**) Electrostatic charge distribution on the surface of Rev1-CT domain (blue is positive, red is negative). Encircled is a pocket on the surface of the domain that accommodates FF residues of RIR motifs of Y-family polymerases.

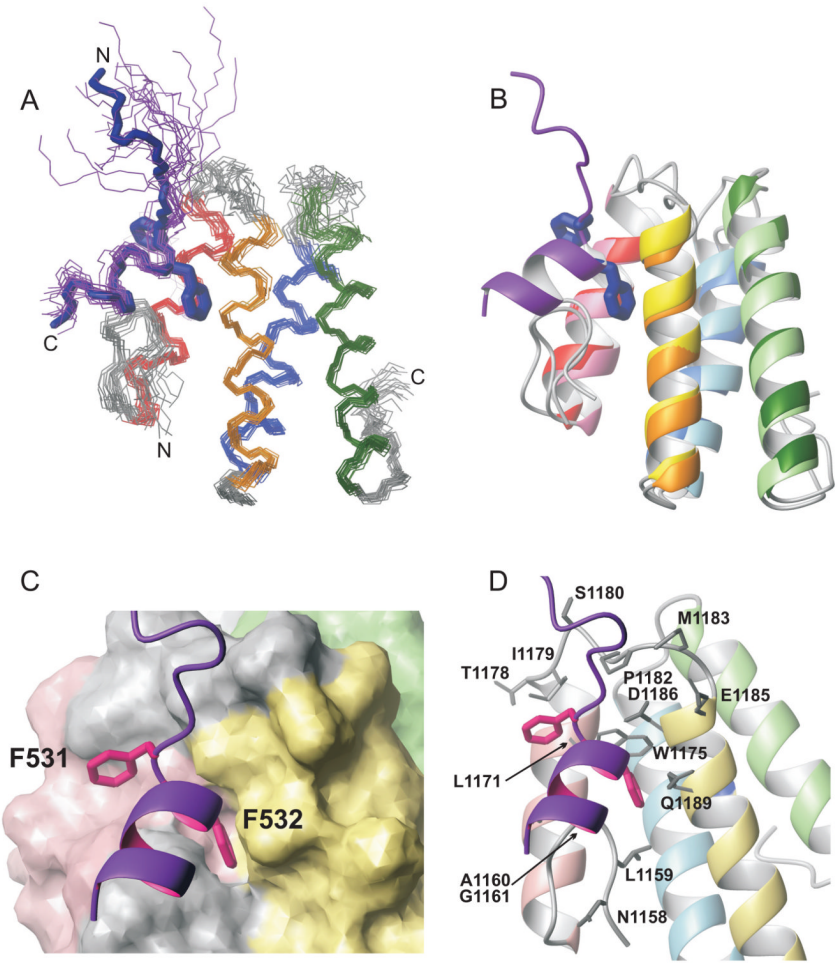

Figure 3.

Spatial structure of the complex of human Rev1-CT domain (residues 1157-1251) with RIR containing peptide from DNA polymerase η (residues 524-539). (**A**) Superposition of the backbone folds of 20 final least energy structures. Also shown are side-chains of Phe 531 and Phe 532 of polη critical for interaction with Rev1-CT. (**B**) Superposition of NMR structures of free Rev1-CT domain (light colors) and Rev1-CT/polη-RIR complex (saturated colors). (**C, D**) Interaction interface of Rev1-CT domain complex with polη-RIR peptide. Side chains of Rev1-CT residues that contribute 5 $Å^2$ or more (averaged over 20 best structures) to intermolecular interaction interface are shown on plot D.

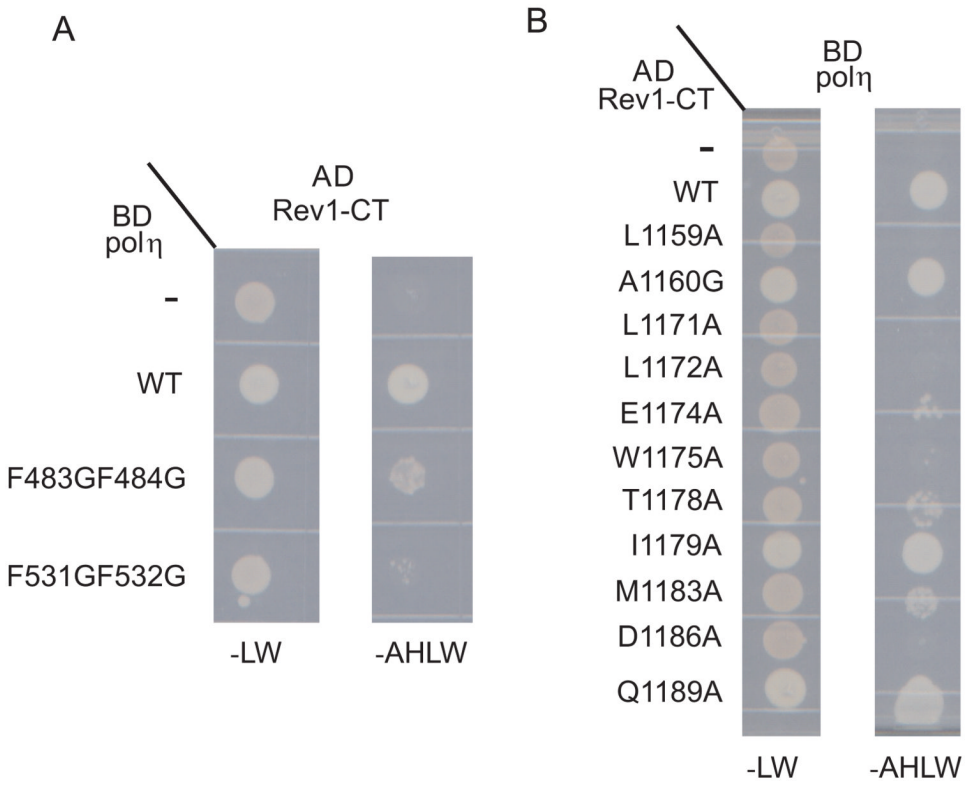

Figure 4.

Mapping of Rev1-CT/polη-RIR interface by yeast two-hybrid assays. The region encoding the human Rev1 C-terminal 120 amino acid fragment (Rev1-CT) was fused to the *GAL4* Activation Domain (AD). The full-length polη-encoding region was appended to the DNA-binding Domain (BD) of *GAL4*. (**A**) Rev1 plasmids were transformed into strains harboring BD-fused wild-type (WT) polη and the indicated mutations or into strains harboring the empty expression plasmids (indicated by the – symbol in the figure). (**B**) AD-appended WT Rev-CT and the indicated mutations were transformed into strains containing BD-WT polη or the empty expression plasmid (-). The plasmids were selected for by growth on media lacking leucine and tryptophan (-LW) and interactions were scored by growth on plates also lacking Adenine and Histidine (-AHLW).

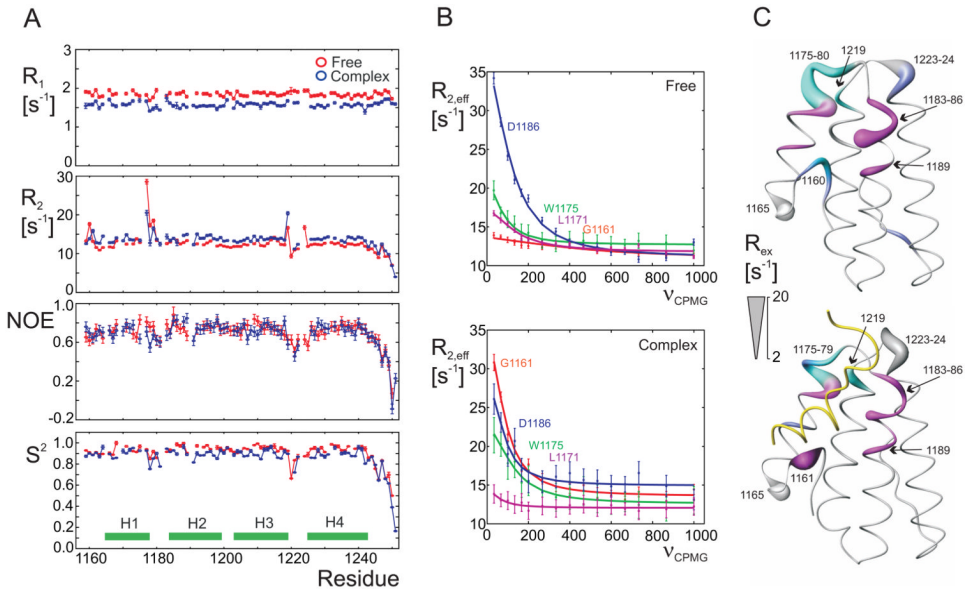

Figure 5.

(**A**) ^{15}N R_1, R_2 relaxation rates and $^{15}N\{^1H\}$ NOE values measured at 11.7 T magnetic field, 15 °C, along with order parameters S^2 (or $S^2 = S_f^2 S_s^2$) for the backbone amide groups obtained in model-free analysis of ^{15}N relaxation data for free Rev1-CT domain (red) and Rev1-CT/polη-RIR complex (blue). (**B**) Examples of experimental ^{15}N CPMG dispersion profiles $R_{2,eff}(\nu_{CPMG})$ measured at 11.7 T magnetic field for selected residues of free (top plot) and polη-RIR bound (bottom plot) forms of Rev1-CT. (**C**) Exchange contributions $R_{ex} = R_{ex,mf}+R_{ex,rd}$ to ^{15}N R_2 rates measured at 11.7 T magnetic field mapped onto structures of free Rev1-CT domain (top) and the complex (bottom). Labeled with numbers are residues with $R_{ex} > 5\ s^{-1}$. Residues exhibiting fast μs-ms time scale exchange identified in model free-analysis of ^{15}N relaxation data[44,56] with $R_{ex,mf}$ contributing over 60% to a total R_{ex} are marked in cyan. Residues displaying slower ms time-scale exchange detected by ^{15}N CPMG dispersion measurements[45,59,60] with $R_{ex,rd}$ contributing over 60% to a total R_{ex} are marked in magenta. Shown in blue are residues with comparable $R_{ex,mf}$ and $R_{ex,rd}$ contributions. Phe 1165, Ser 1223 (free domain and the complex) and Val 1224 (the complex only) whose resonances are not detected in NMR spectra presumably due to severe μs-ms exchange line-broadening are assumed high R_{ex} values and are marked in grey.

Table 1

NMR-based restraints used for structure calculation of Rev1-CT domain and Rev1-CT/polη-RIR complex, and structure refinement statistics.

	Free Rev1-CT	Rev1-CT/polη complex	
Summary of restraints			
Total NOE distance restraints	1853	1526	
Short range(|i-j| <=1)	1013	856/53[a]	
Medium range(1<|i-j|<5)	468	315/9[a]	
Long range (|i-j|>=5)	372	221/0[a]	
Intermolecular	-	51/21[b]	
Dihedral angles restrains (φ and ψ)	180	152/26[a]	
Hydrogen bonds	46	40/4[a]	
Structure refinement statistics			
Deviation from NMR-based restraints			
NOE (Å)	0.02	0.02	
Dihedral restraints (degrees)	1.1	1.3	
Deviation from idealized geometry			
Bonds (Å)	0.02	0.02	
Angles (degrees)	1.1	1.2	
Ramachandran plot favorable	90.1%	90.3%	
RMSD, pairwise (Å)			
All residues		Rev1-CT	polη-RIR
Backbone atoms	0.87±0.16	1.08±0.19	2.58±1.03
Heavy atoms	1.35±0.14	1.83±0.23	3.40±1.00
Residues in regular secondary structure elements[c]			
Backbone atoms	0.53±0.11	0.62±0.12	0.27±0.08
Heavy atoms	1.08±0.10	1.51±0.22	1.38±0.26

[a] intra-molecular restraints for Rev1-CT/polη peptide

[b] upper/low distance restraints

[c] residues 1165-1178, 1184-1199, 1203-1219, 1224-1243 in Rev1-CT, 532-539 in polη.